Scheme II

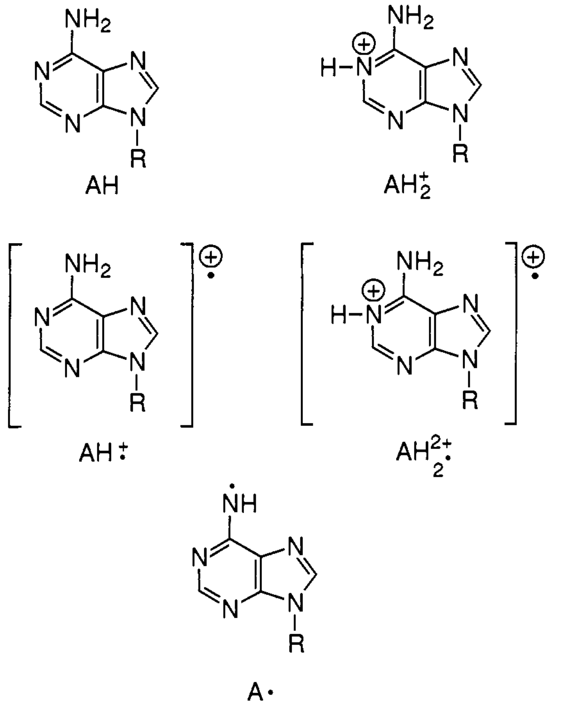

10.0 and 3.0 mT, respectively, on the basis of values for J_0 and α obtained from simulation of field-dependent CIDNP experiments on polymethylene biradicals.[16a,18] However, in applying eq 4 and 5 several assumptions are involved, such as the exclusive r dependence of the exchange integral and the fact that we have delocalized radicals in contrast to the ketone derived radicals used as calibration. Therefore, in view of these uncertainties the distances mentioned should be considered only as rough estimates.

Conclusions

The high-field photo-CIDNP spectrum of FAD at acid pH is similar to that obtained from 5′-AMP and free flavin Fl and can be explained by T_0–S mixing in a biradical formed by intramolecular electron transfer from the adenine to the triplet flavin moiety.

The pH dependence shows a pronounced maximum at pH 2.4 and is very similar to the pH dependence of the fluorescence of FAD. At low pH the decrease in both fluorescence and CIDNP probably has the same origin, i.e., the radiationless decay of the excited singlet of flavin. At high pH the decrease in CIDNP is due to a shift from the protonated form of the biradical $FH^\bullet$–$AH^{\bullet+}$ to the neutral form $FH^\bullet$–$A^\bullet$ with concomitant increased stacking interactions (and therefore strong exchange interaction) in the neutral form. The pH-dependent curve follows the pK_a of ground-state FAD (protonation of the adenine moiety), because the protonation–deprotonation equilibria are slow on the CIDNP time scale except for intramolecular proton transfer, reaction 4 in Scheme I.

CIDNP experiments at low magnetic field carried out with a specially designed falling tube system showed that the polarization at low field arises from T_-–S mixing in the biradical with the same pH dependence as that observed at high field. The field-dependent CIDNP curves in the acid pH region show two maxima at 3.0 and 10.0 mT corresponding to two open (destacked) conformations of the biradical $FH^\bullet$–$AH^{\bullet+}$, which interconvert slowly on the CIDNP time scale.

Acknowledgment. We thank Dr. F. de Kanter (Free University, Amsterdam) for his advice concerning the design and construction of the magnetic field dependent setup and Dr. F. Müller (Sandoz, Basel) and Dr. R. M. Scheek (University of Groningen) for helpful discussions. Expert technical assistance by K. Dijkstra and M. de Rapper is gratefully acknowledged. This work was supported by the Netherlands Foundation for Chemical Research (SON) with financial aid from the Netherlands Organization for Scientific Research (NWO).

Intermolecular Resonance Coupling of Solute and Solvent Vibrational Modes

C. Veas and J. L. McHale*

Contribution from the Department of Chemistry, University of Idaho, Moscow, Idaho 83843.
Received January 23, 1989

Abstract: A theoretical derivation is presented of vibrational resonance coupling (Fermi resonance) between a solute Raman mode and the collective vibrational excitation of N equivalent surrounding solvent molecules. The perturbed intensities and frequencies of the coupled vibrations are shown to depend on the number of molecules in the solvation sphere. The effect of this sort of vibrational coupling on resonance Raman excitation profiles is considered, and it is shown that the effect has the potential to reveal the number of perturbing solvent molecules. The theory is applied to the analysis of previously reported resonance Raman data on cobalt porphyrin complexes.

I. Introduction

In Raman spectroscopy, intensity borrowing between vibrational modes on different molecules can result from vibrational coupling in the ground electronic states or from coupling of the excited electronic states responsible for the Raman intensity. The former effect, which is the subject of this paper, requires a close match of the vibrational energy levels and an appropriate dependence of the intermolecular potential on the normal coordinates for the two vibrational modes. Unlike intramolecular Fermi resonance,[1] which involves coupling between a fundamental and an overtone or combination vibration, intermolecular Fermi resonance can involve the interaction of fundamentals on two different molecules. The reason for the difference is that the coupling of two fundamentals is made possible by a perturbation of the type $(\partial^2 V/$

---

(1) (a) Fermi, E. Z. *Z. Physik.* **1931**, *71*, 250. (b) Herzberg, G. *Molecular Spectra and Structure*; Van Nostrand Reinhold: New York, 1945; Vol. II, pp 215–217.

$\partial Q_A \partial Q_B$), where Q_A and Q_B are normal coordinates and V is potential energy. This sort of derivative vanishes when Q_A and Q_B are normal coordinates on the *same* molecule but not when they are normal coordinates of *different* molecules.

Although intermolecular effects on intramolecular Fermi resonance have been observed experimentally[2-4] and described theoretically,[5] intermolecular vibrational coupling between unlike molecules has not, to our knowledge, been extensively considered theoretically. (See, however, ref 6 for a very general treatment of Fermi resonance interaction of arbitrary vibrational states.) Recently, some very interesting effects of vibrational coupling have been observed for ligand vibrations in the resonance Raman spectra of O_2 adducts of cobalt porphyrin complexes.[7-10] Intensity borrowing in resonance Raman spectroscopy is particularly interesting because dramatic changes in the Raman intensity of a chromophoric solute can lead to unexpected excitation profiles for the vibrational modes of the solvent. In view of the widespread practice of measuring relative Raman intensities by referencing the intensity of the solute mode to that of a nearby solvent mode (in order to minimize differential self-absorption of scattered light), the problem is of considerable practical interest. In this paper, we present the derivation of the perturbed intensities and frequencies for the case of a single solute interacting with N equivalent solvent molecules. We show how the working equations may be used to obtain the uncoupled frequencies and intensities, and possibly the number of molecules in the solvation sphere.

II. Theory

Consider a single molecule (A) surrounded by N solvent molecules (B). A vibrational mode ν_A of the solute is close in frequency to a mode ν_B of the solvent. A zeroth-order vibrational wave function of the aggregate can be expressed as the $(N+1)$-fold product of the harmonic oscillator wave function for molecule A and N such wave functions for the solvent molecules B. The zeroth-order ground-state wave function is

$$\Psi_g^{(0)} = |\chi_A{}^0\chi_1{}^0\chi_2{}^0...\chi_N{}^0\rangle \tag{1}$$

where $\chi_A{}^\vartheta(\chi_i{}^\vartheta)$ is the harmonic oscillator wave function for the ϑth vibrational state of molecule A (or of the ith solvent molecule). The ground-state energy is

$$E_g^{(0)} = {}^1\!/_2 h\nu_A + \frac{N}{2}h\nu_B \tag{2}$$

The excited state describing a single quantum of vibrational excitation in the aggregate is written as a linear combination of product wave functions, where one of the $N+1$ molecules is found in the $\vartheta = 1$ state:

$$\Psi_e = C_A|\chi_A{}^1\chi_1{}^0\chi_2{}^0...\chi_N{}^0\rangle + C_1|\chi_A{}^0\chi_1{}^1\chi_2{}^0...\chi_N{}^0\rangle + ... + C_N|\chi_A{}^0\chi_1{}^0\chi_2{}^0...\chi_N{}^1\rangle \tag{3}$$

The coefficients $C_A, C_1, ..., C_N$ are to be determined variationally. The Hamiltonian for the aggregate is

$$\hat{H} = \hat{H}_A + \sum_B \hat{H}_B + \hat{H}' \tag{4}$$

where

$$\hat{H}_A\chi_A{}^\vartheta = (\vartheta + {}^1\!/_2)h\nu_A\chi_A{}^\vartheta \tag{5}$$

$$\hat{H}_B\chi_B{}^\vartheta = (\vartheta + {}^1\!/_2)h\nu_B\chi_B{}^\vartheta \quad B = 1, 2, ..., N$$

The perturbation $\hat{H}'$ is the intermolecular "anharmonicity", which is responsible for the coupling:

$$\hat{H}' = \sum_{B=1}^{N} VQ_AQ_B \qquad \text{where } V = \left.\frac{\partial^2 V_{AB}}{\partial Q_A \partial Q_B}\right|_{\{Q\}} = 0 \tag{6}$$

V_{AB} is the intermolecular potential and Q_A and Q_B are the normal coordinates. The perturbed excited-state energies are the roots of the following secular determinant:

$$\det\begin{bmatrix} H_{AA} - E & H_{A1} & H_{A2} & \dots & H_{AN} \\ H_{A1} & H_{11} - E & H_{12} & \dots & H_{1N} \\ \vdots & & \vdots & & \vdots \\ H_{AN} & H_{1N} & H_{2N} & \dots & H_{NN} - E \end{bmatrix} = 0 \tag{7}$$

The perturbation $\hat{H}'$ does not contribute to the diagonal elements

$$\begin{aligned} H_{AA} &= \langle\chi_A{}^1\chi_1{}^0\chi_2{}^0...\chi_N{}^0|\hat{H}_A + \hat{H}_B|\chi_A{}^1\chi_1{}^0\chi_2{}^0...\chi_N{}^0\rangle \\ &= \frac{3}{2}h\nu_A + \frac{N}{2}h\nu_B \end{aligned} \tag{8}$$

and

$$\begin{aligned} H_{ii} &= \langle\chi_A{}^0\chi_1{}^0...\chi_i{}^1...\chi_N{}^0|\hat{H}_A + \hat{H}_B|\chi_A{}^0\chi_1{}^0...\chi_i{}^1...\chi_N{}^0\rangle \\ &= H_{11} = H_{22} = ...H_{NN} \equiv H_{BB} \\ &= \frac{1}{2}h\nu_A + \left(\frac{N}{2} + 1\right)h\nu_B \end{aligned} \tag{9}$$

The off-diagonal elements, on the other hand, derive from the perturbation. Matrix elements connecting states with one quantum of excitation on different solvent molecules are assumed to vanish. (In other words, resonance coupling of solvent vibrational modes, such as that leading to a splitting of polarized and depolarized peak frequencies,[11] is neglected.) The nonzero off-diagonal matrix elements are thus:

$$\begin{aligned} H_{A1} = H_{A2} = ...H_{AN} &= V\left(\frac{h}{8\pi^2 m_A\nu_A}\right)^{1/2}\left(\frac{h}{8\pi^2 m_B\nu_B}\right)^{1/2} \\ &\equiv U \end{aligned} \tag{10}$$

In eq 10, m_A and m_B are the effective masses for the vibrational modes, and the coupling strength U has been defined to have units of energy.

The solution to eq 7 leads to $N - 1$ roots for the energy that are unperturbed ($E = H_{BB}$) and two roots that are perturbed. The two perturbed roots are

$$E_\pm = {}^1\!/_2\{H_{AA} + H_{BB} \pm [(H_{AA} - H_{BB})^2 + 4NU^2]^{1/2}\} \tag{11}$$

When the zeroth-order frequency difference is defined as $\Delta = h(\nu_A - \nu_B)$, the following expression for the two perturbed frequencies is obtained:

$$\nu_\pm = {}^1\!/_2\{(\nu_A + \nu_B) \pm h^{-1}(\Delta^2 + 4NU^2)^{1/2}\} \tag{12}$$

In the limit that the coupling U is small compared to the splitting Δ, the perturbed frequencies are given by

$$\nu_+ = \nu_A + \frac{NU^2}{h\Delta} \qquad \nu_- = \nu_B - \frac{NU^2}{h\Delta} \tag{13}$$

As usual in Fermi resonance, the interacting states repel each other. (Note that $\nu_+ > \nu_-$ if Δ is positive, as will be assumed throughout the paper for convenience.) Although the weak coupling limit is mathematically convenient, it does not necessarily hold in general, as will be shown in the examples of section III. However, it is always true that the sum of the perturbed frequencies is equal to that of the unperturbed frequencies, a fact that can be exploited to determine whether vibrational resonance coupling is at work in an observed spectrum and to calculate the uncoupled frequencies ν_A and ν_B.

In order to evaluate the Raman intensities of the perturbed modes, we consider the coefficients $C_A{}^\pm, C_1{}^\pm, ..., C_N{}^\pm$, which

---

(2) Schwarz, M.; Wang, C. H. *J. Chem. Phys.* **1973**, *59*, 5258.

(3) Lundeen, J. W.; Koehler, W. H. *J. Phys. Chem.* **1975**, *79*, 2957.

(4) Koehler, W. H.; Lundeen, J. W.; Moradi-Araghi, A.; de Bettignies, B.; Schultz, L. D.; Schwarz, M. *J. Phys. Chem.* **1979**, *83*, 3264.

(5) McHale, J. L.; Wang, C. H. *J. Chem. Phys.* **1980**, *73*, 3600.

(6) Monecke, J. *J. Raman Spectrosc.* **1987**, *18*, 477.

(7) Bajdor, K.; Kincaid, J. R.; Nakamoto, K. *J. Am. Chem. Soc.* **1984**, *106*, 7741.

(8) Kincaid, J. R.; Proniewicz, L. M.; Bajdor, K.; Bruha, A.; Nakamoto, K. *J. Am. Chem. Soc.* **1985**, *107*, 6775.

(9) Proniewicz, L. M.; Nakamoto, K.; Kincaid, J. R. *J. Am. Chem. Soc.* **1988**, *110*, 4541.

(10) Bruha, A.; Kincaid, J. R. *J. Am. Chem. Soc.* **1988**, *110*, 6006.

(11) Wang, C. H.; McHale, J. L. *J. Chem. Phys.* **1980**, *72*, 4039.

describe the two perturbed excited vibrational states, $\Psi_e^{\pm}$. The coefficients $C_1^{\pm}$ through $C_N^{\pm}$ are all equal, so we define these as $C_B^{\pm}$. The necessary coefficients are

$$C_A^+ = \left[\frac{N^2U^2}{N^2U^2 + \dfrac{N}{4}(\Delta - D)^2}\right]^{1/2} \tag{14a}$$

$$C_B^+ = \left[\frac{\frac{1}{4}(\Delta - D)^2}{N^2U^2 + \dfrac{N}{4}(\Delta - D)^2}\right]^{1/2} \tag{14b}$$

where $D \equiv (\Delta^2 + 4NU^2)^{1/2}$. In the weak coupling limit, these go over to

$$C_A^+ \approx \left[\frac{\Delta^2}{\Delta^2 + NU^2}\right]^{1/2} \approx 1 - \frac{NU^2}{\Delta^2} \tag{15a}$$

$$C_B^+ \approx \left[\frac{U^2}{\Delta^2 + NU^2}\right]^{1/2} \approx \frac{U}{\Delta} \tag{15b}$$

The coefficients of the lower energy state are related to C_A^+ and C_B^+ by

$$(C_A^-)^2 = N(C_B^+)^2 \qquad (C_B^-)^2 = (C_A^+)^2/N \tag{16}$$

also

$$C_A^-C_B^- = -C_A^+C_B^+ \tag{17}$$

The intensities of the two perturbed modes are determined by

$$I_{\pm} = |\langle\Psi_g^{(0)}|(\alpha_A Q_A + \sum_{B=1}^{N}\alpha_B Q_B)|\Psi_e^{\pm}\rangle|^2 \tag{18a}$$

For example, the intensity of the higher frequency mode can be written as

$$I_+ = (C_A^+)^2\alpha_A^2 + N^2(C_B^+)^2\alpha_B^2 + 2NC_A^+C_B^+\alpha_A\alpha_B \tag{18b}$$

and similarly for I_-, with C_A^+ and C_B^+ replaced by C_A^- and C_B^-. Because of eq 17 and normalization ($C_A^2 + NC_B^2 = 1$), the cross term in $\alpha_A\alpha_B$ cancels when I_+ and I_- are added together, leading to

$$I_+ + I_- = \alpha_A^2 + N\alpha_B^2 \tag{19}$$

Thus, the total intensity, integrated over both of the perturbed bands, is rigorously unchanged by the solvent–solute interaction; one band must increase in intensity at the expense of the other. Which band increases in intensity is determined by the sign of the coupling parameter U and of the unperturbed polarizability derivatives α_A and α_B.

If the perturbation of the frequencies is very small, which is to be expected for the weak coupling case, $|U/\Delta| \ll 1$, then it may be impossible to observe the perturbed solvent peak in the presence of the much larger peak due to bulk solvent molecules. In this case, assuming that ν_- and ν_B cannot be resolved, the experimentally observed intensity I_- is the sum of three contributions: that due to the bulk solvent, the unperturbed intensity contributed by the N molecules in the solvation sphere (in other words, the $N - 1$ roots with unperturbed intensity α_B^2), and the perturbed intensity due to the molecules in the solvation sphere. When N_A and N_B represent the formal concentrations of solute and solvent, the total intensity due to the solvent is given by

$$I_-(\text{exp}) = (N_B - NN_A)\alpha_B^2 + N_A(N - 1)\alpha_B^2 + N_A I_- \tag{20a}$$

and that due to the solute is just

$$I_+(\text{exp}) = N_A I_+ \tag{21}$$

Thus the total intensity integrated over both peaks is

$$I_+(\text{exp}) + I_-(\text{exp}) = N_A\alpha_A^2 + [N_B + N_A(N - 1)]\alpha_B^2 \tag{22}$$

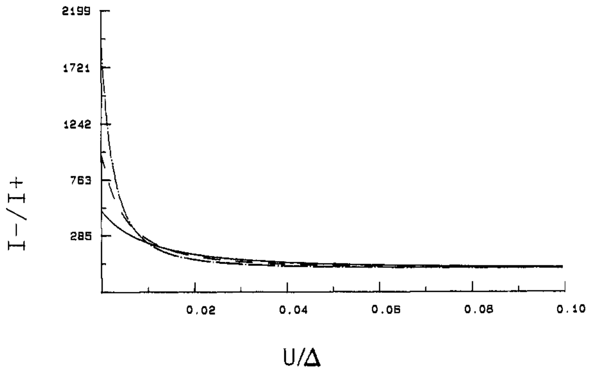

Figure 1. I_-/I_+ as a function of $|U/\Delta|$ for the positive cross term case (see text) and for $|\alpha_A/\alpha_B| = 0.1$, for solvation numbers $N = 5$ (—), $N = 10$ (---), and $N = 20$ (–·–).

Equation 21 implies that solvation by N molecules leads to an increase in total intensity of the two bands, by an amount proportional to the solvation number minus 1. This is similar to the Raman intensity enhancement induced by aggregation considered by Akins.[12] The result suggests a simple experiment to determine the solvation number N in a mixed-solvent system. Suppose a binary solvent, say B plus C, could be found, where B has a vibrational mode close in frequency to a mode of A but C does not. After the relative intensities of A and B are determined separately in solvent C, eq 22 could be used to determine the aggregation number N in a solution of A in B plus C. To be practical, fairly high concentrations of A relative to B would be required.

To demonstrate that even weak coupling can lead to measurable intensity changes, consider the intensity ratio I_+/I_- of the separate peaks, according to eq 18. If the coupling U is positive, the coefficients C_A^+ and C_B^+ will have the same sign, whereas negative U will lead to opposite signs for C_A^- and C_B^-. Taking $\Delta > 0$, the ratio C_B^+/C_A^+ is equal to $(D - \Delta)/2NU$ in either case. Thus, the ratio of the intensity of the higher frequency peak to that of the lower frequency peak is

$$\frac{I_+}{I_-} = \frac{\left[\alpha_A + \dfrac{D - \Delta}{2U}\alpha_B\right]^2}{N\left[\alpha_B - \dfrac{D - \Delta}{2NU}\alpha_A\right]^2} \tag{23}$$

The change in intensity due to coupling, considered as a function of the absolute value of U/Δ, depends on the signs of U, α_A, and α_B as well as on the magnitude of the ratio of the unperturbed polarizabilities. In the discussion that follows, Δ is arbitrarily assumed to be positive so that the influence of the sign and magnitude of the other parameters can be considered. Note that for coupling U, which is very small compared to the splitting Δ, D is approximately equal to Δ and the intensity ratio (as well as the frequencies) are unperturbed.

In Figures 1–4 are shown some examples of how the intensity ratio varies with the magnitude of U/Δ for various values of the polarizability ratio. For each value of α_A/α_B we consider two possibilities for the sign of the cross term in eq 23. For a positive cross term (Figures 1 and 3), either $U > 0$ and α_A and α_B have the same sign or $U < 0$ and α_A and α_B have opposite signs. In this case the intensity I_- of the lower frequency peak can vanish when the absolute values of α_B/α_A and $(D - \Delta)/2NU$ are equal. Conversely, in the case of a negative cross term (Figures 2 and 4), where $U < 0$ and α_A and α_B have the same sign or $U > 0$ and α_A and α_B have opposite signs, the intensity I_+ can vanish when $|\alpha_B/\alpha_A| = |(D - \Delta)/2U|$. (Note that we plot I_-/I_+ in Figures 1 and 3 and I_+/I_- in Figures 2 and 4.) Thus, it is possible to have very dramatic changes in the intensity ratio even for very weak coupling, $|U/\Delta| \ll 1$, particularly when $\alpha_A \gg \alpha_B$, as in the case where the Raman mode of A is resonance enhanced.

---

[12] Akins, D. L. *J. Phys. Chem.* **1986**, *90*, 1530.

Table I. Fermi Resonance Data for Co(TPP-d_8)DCP(O_2) (cm^{-1})[a]

	ν_+	ν_-	$\nu_A(O_2)$	ν_B(DCP)	Δ	$\lvert U\rvert$
$^{16}O_2$	1160	1112	1158 ± 5	1114 ± 5	43 ± 10	10.7 ± 12
$^{16}O^{18}O$	1132 (1132 ± 12)	1108 (1108 ± 12)	1126 ± 23	1114 ± 5	12 ± 22	10.5 ± 12
$^{18}O_2$	1121 (1118 ± 6)	1086 (1083 ± 6)	1086 ± 10	1114 ± 5	−21 ± 11	10.4 ± 12

[a] Calculated values of ν_+ and ν_- are in parentheses.

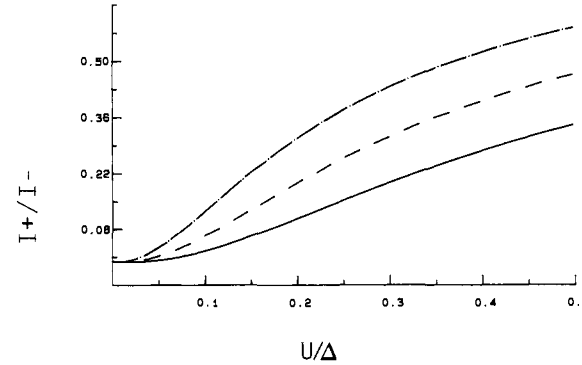

Figure 2. As for Figure 1, except for a negative cross term, and I_+/I_- is plotted.

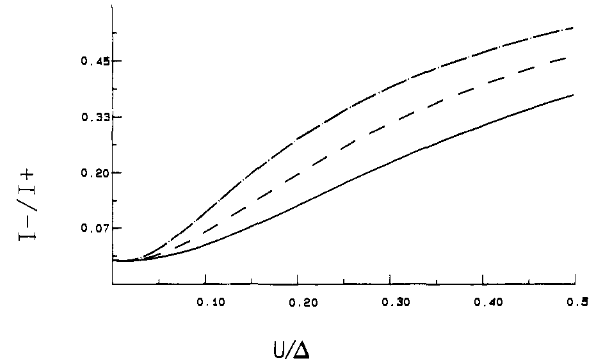

Figure 3. As for Figure 1 but with $|\alpha_A/\alpha_B| = 100$.

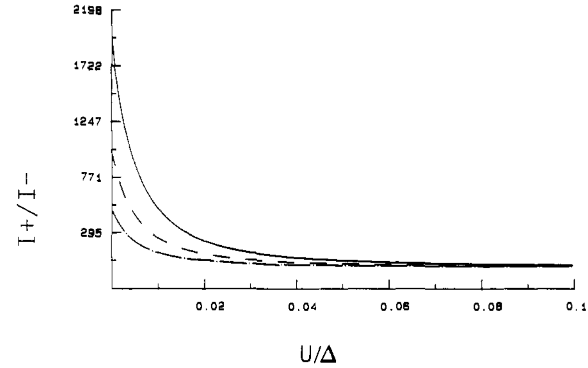

Figure 4. As for Figure 2 but with $|\alpha_A/\alpha_B| = 100$.

Since measurable intensity changes are possible for weak coupling, the perturbed solvent peak may not be resolved from that due to bulk solvent. In this case, the experimental intensity ratio is given by

$$\frac{I_+(\text{exp})}{I_-(\text{exp})} = \frac{N_A\left(\alpha_A + \frac{D-\Delta}{2U}\alpha_B\right)^2}{N_A N\left(\frac{D-\Delta}{2NU}\alpha_A - \alpha_B\right)^2 + (N_B - N_A)\alpha_B^{\,2}} \tag{24}$$

Equation 24 predicts an unexpected frequency dependence of the solvent Raman intensity in the case where a nearby solute mode undergoes resonance enhancement. If the term $(D-\Delta)/2NU$ is comparable to the ratio of the polarizability derivatives, α_B/α_A, then the excitation profile of the solvent Raman mode will contain some of the frequency dependence of the Raman mode of the solute.

Table II. Rough Estimates of Intensity Ratios in Co(TPP-d_8)DCP(O_2)

	$(D-\Delta)/2U$	I_+/I_- obsd	I_+/I_- pred	$\lvert\alpha_B/\alpha_A\rvert$
$^{16}O_2$	0.23	~3:1		~0.30
$^{16}O^{18}O$	0.58	~1:1	0.9	
$^{18}O_2$	0.40	~1:3	0.7	

III. Examples

As an illustration of how the formalism can be used to decouple Fermi resonance doublets, we examine the Raman data of Kincaid et al.,[8] who studied a series of complexes Co(TPP-d_8)(DCP)O_2 with three different isotopes of dioxygen. TPP is tetraphenylporphyrin and DCP is 3,5-dichloropyridine. The first two columns in Table I show the resonance Raman data reported in ref 9 for the $^{16}O_2$, $^{16}O^{18}O$, and $^{18}O_2$ complexes. The authors assign the less intense peak at 1112, 1108, and 1121 cm^{-1}, respectively, to a vibrational mode of DCP, which borrows intensity from the O–O stretch at 1160, 1132, and 1086 cm^{-1}. When eq 12 is used with $N = 1$, it is easy to show that this interpretation is quantitatively consistent with the data. Without making any assumption about the isotope ratios of the dioxygen stretch, $\nu(^{16}O-^{16}O):\nu(^{16}O-^{18}O):\nu(^{18}O-^{18}O)$, the values of ν_+ and ν_- for the $^{16}O_2$ and $^{16}O^{18}O$ complexes were used to find $\Delta = \nu_A(^{16}O_2) - \nu_B(\text{DCP}) = 43$ cm^{-1}, $\nu_A(^{16}O_2) = 1157.5$ cm^{-1}, $\nu_B(\text{DCP}) = 1114.5$ cm^{-1}, and $|U| = 10.7$ cm^{-1}. The value of ν_B is assumed to be independent of the O_2 isotope, and the value of $|U|$ was corrected for reduced mass (see eq 10) to arrive at the values given in the last column of Table I. The experimental splitting $\nu_+ - \nu_-$ was then used to calculate Δ and ν_A. Although the ±1-cm^{-1} error in ν_+ and ν_- leads to rather large propagated errors in Δ and $|U|$, the calculated isotope ratios of the uncoupled O–O stretch, $\nu(^{16}O-^{16}O):\nu(^{16}O-^{18}O):\nu(^{18}O-^{18}O) = 1.0:0.97:0.94$, are in good agreement with the ratios expected on the basis of the reduced mass of free dioxygen. Furthermore, the calculated values of ν_+ and ν_-, given in parentheses, are found to agree closely with the experimental numbers. Thus the idea of intermolecular Fermi resonance is entirely consistent with the author's data. The approach presented here can be used to decouple Fermi doublets in order to assess the importance of steric or electronic factors that might perturb the frequency of a ligand vibration.

The values of Δ and $|U|$ given in Table I can be used to predict the intensity ratio of the coupled peaks, according to eq 23. When very rough estimates of the observed intensity ratios shown in Figure 1 of ref 9 are used, it is possible to calculate the uncoupled polarizability ratio $|\alpha_B/\alpha_A|$ from the data for one isotopomer and use it to predict the intensity ratios for the other two. As shown in Table II, the magnitude of the intensity borrowing is predicted to be smallest in the $^{16}O_2$ isotopomer and greatest in the $^{16}O^{18}O$ isotopomer. This is qualitatively in accord with the spectra of ref 9, where the intensity of the DCP peak is shown to increase relative to that of O_2 in the order $^{16}O_2$, $^{18}O_2$, $^{16}O^{18}O$. If the intensity ratio I_+/I_- is guessed to be about 3:1 for the $^{16}O_2$ complex, this leads to $|\alpha_B/\alpha_A| \approx 0.3$. The predicted values of I_+/I_- for the $^{16}O^{18}O$ and $^{18}O_2$ complexes are then calculated using eq 23, giving the numbers in the third column of Table II. This is a crude calculation, not only because the experimental intensity ratios are uncertain but also because of the large uncertainties in $|U|$ and Δ that result from propagating the ±1-cm^{-1} uncertainty in the experimental frequencies. Nevertheless, the qualitative trends in the observed intensity ratios are in good agreement with the theory.

The above example is really intermediate between intra- and intermolecular vibrational resonance coupling, since the coupled vibrations are localized on different ligands of the same molecular complex. However, coupling of fundamental vibrations of different ligands is allowed because $(\partial^2 V/\partial Q_A \partial Q_B)$ is not required to be zero. As expected, the weak coupling limit is not valid (and was not used), since the absolute values of the coupling parameter U are not small compared to those of the unperturbed frequency difference Δ. In ref 8 is reported an example of intermolecular Fermi resonance, which illustrates that intensity borrowing and frequency shifts can still be observed in more weakly coupled systems. As reported by Kincaid et al.,[8] in CH_2Cl_2 solutions containing pyridine, the $^{16}O{-}^{16}O$ stretch of Co(TPP-d_8)O_2 is observed at 1143 cm^{-1}, along with an enhanced solvent mode at 1155 cm^{-1}. In CD_2Cl_2 solution, the $^{16}O_2$ vibration was found at 1148 cm^{-1}, and the 1155-cm^{-1} mode disappeared. These numbers imply a coupling parameter $|U| = 5.9$ cm^{-1}, which is smaller than the values given in Table I for interligand coupling. However, the uncoupled frequencies are $\nu(^{16}O_2) = 1148$ cm^{-1} and $\nu(CH_2Cl_2) = 1150$ cm^{-1}, so $|U|$ is not small compared to $|\Delta| = 2$ cm^{-1}. If the frequency shift for the complex with $^{18}O_2$ is evaluated, it is found to be negligible, due to the much larger value of $|\Delta|$, 61 cm^{-1}. The intensity borrowing is correspondingly weak, since $(D - \Delta)/2U$ (see eq 23) is only about 0.07. Thus in the case of the $^{18}O_2$ complex, the theoretical prediction of negligible solvent enhancement or O_2 frequency shift is in agreement with the experimental results.

IV. Conclusion

A simple theory of intermolecular vibrational resonance coupling has been presented and has been shown to be valid for the strong coupling observed in a molecular complex. Frequency shifts and intensity perturbations may be observed for any general type of intermolecular interaction, provided there is a dependence of the intermolecular potential on the normal coordinates of the coupled vibrational modes. In the case of intermolecular coupling involving a solute surrounded by a solvation sphere, an experimental approach is suggested for determining solvation numbers from resonance Raman spectra in a mixed solvent. An important conclusion is that intensity perturbations can result even in the weak coupling case, where a frequency shift cannot be observed, especially in the case of resonance enhancement of the solute Raman mode.

One limitation of the derivation is that all the interacting solvent molecules are considered equivalent. The intermolecular coupling U is actually a function of distance and relative orientation. The distance dependence, incidently, was illustrated very nicely in ref 7, where the solvent intensity borrowing was shown to vanish for the very hindered picket-fence porphyrin adduct. However, if U is averaged over an equilibrium distribution of solvent coordinates, then it is the same for every solute–solvent pair, and the approximation of equivalent solvent molecules is valid. Further experiments to determine the utility of the proposed approach for determining solvation numbers are in progress.

Acknowledgment. The support of this work by NSF Grant CHE-8605079 is gratefully acknowledged.

Proposed Structure for the Prosthetic Group of the Catalase HPII from *Escherichia coli*

Jen Ting Chiu,[†] Peter C. Loewen,[‡] Jacek Switala,[‡] Robert B. Gennis,[§] and Russell Timkovich*[,†]

Contribution from the Department of Chemistry, University of Alabama, Tuscaloosa, Alabama 35487-0336, the Departments of Chemistry and Biochemistry, University of Illinois, Urbana, Illinois 61801, and the Department of Microbiology, University of Manitoba, Winnipeg, Manitoba R3T 2N2, Canada. *Received March 6, 1989*

Abstract: *Escherichia coli* contains two catalases designated HPI and HPII. The heme prosthetic group of HPII is an unusual green chromophore that was believed to be a member of the family of *d*-type hemes. The heme was extracted and compared to the heme of the terminal oxidase cytochrome complex in *E. coli*. The two hemes were very similar by visible spectroscopy but were resolved by chromatography. The heme was converted to a free-base, esterified derivative that was characterized by ^1H NMR spectroscopy, infrared spectroscopy, and mass spectrometry. The proposed structure for the free base is 12-hydroxy-13-*cis*-spirolactone-2,7,12,18-tetramethyl-3,8-divinyl-17-propionylporphyrin.

The respiratory electron-transport chain of certain aerobic bacteria contains an unusual prosthetic group for the terminal oxidase. This group, originally called heme a_2 but later renamed to heme *d*, is the oxygen, carbon monoxide binding site. It is spectroscopically characterized by a red shift of the α band in the visible spectrum. In 1956 Barrett[1] extensively investigated the properties of heme a_2 and the porphyrin derived by iron removal and tentatively proposed that it was a dihydroporphyrin. In 1985 it was shown by isolation and purification of the chlorin derived from the heme of the terminal oxidase in *E. coli* that the basic structure was analogous to that of protoporphyrin IX but that ring C contained extra oxygen functional groups.[2] The demetalized free base actually characterized was a hydroxyl, spirolactone form, **1** (Chart I). It was pointed out that this final product could have arisen from spontaneous cyclization of a diol **3**. Later infrared analysis of freshly prepared heme extracts indicated that a diol was directly obtainable from the haloenzyme.[3] The proposed structure for the natural product was confirmed by a total synthesis by Sotiriou and Chang.[4] The total synthesis also

---

[†] University of Alabama.

[‡] University of Manitoba.

[§] University of Illinois.

* To whom correspondence should be addressed.

(1) Barrett, J. *Biochem. J.* **1956**, *64*, 626–639.

(2) Timkovich, R.; Cork, M. S.; Gennis, R. B.; Johnson, P. Y. *J. Am. Chem. Soc.* **1985**, *107*, 6069–6075.

(3) Vavra, M. R.; Timkovich, R.; Yap, F.; Gennis, R. B. *Arch. Biochem. Biophys.* **1986**, *250*, 461–468.

0002-7863/89/1511-7046$01.50/0